

Ski Lift Tower Mounted Solar Panels

Michael Beske-Somers

Louis Chailleux

Lyle Cordes

Charles Dubrule

Department of Mechanical Engineering
The University of Vermont
ME 2310 A: Final Design Project

May 4, 2024

Contents

1	Project Description	3
2	Safety and Ethics	6
2.1	Structural Safety	6
2.2	Breakaway System Safety	6
2.3	Ethics	7
3	Component Designs	8
3.1	Solar Panel Specifications	10
3.2	Snow Load	13
3.3	Tower	13
3.4	Horizontal Structure	14
3.5	Hinge and Breakaway System	16
4	Finite Element Analysis	22
4.1	Tower FEA	22
4.2	Horizontal Structure FEA	23
4.3	Wind Simulation	24
5	Appendix	26
5.1	Sample Calculations	26
5.2	Finite Element Analysis Results	27
6	Bibliography	41

1 Project Description

This system is intended to produce renewable power for ski areas with minimal to no disruption to their existing operations. The current ski lift tower is adapted to hold four solar panels, totalling 8 m^2 and approximately 83 kg .¹ Two of the panels are mounted at an angle on top of the tower in an A-frame configuration. The other two panels are placed on the underside of the tower to face the ground and capitalize on the light being reflected off of the snow. A sketch of the original design is displayed below in Figure 1. While the final design mostly resembles this original sketch, the upside down solar panels in the final design are attached to the horizontal structure instead of the tower itself.

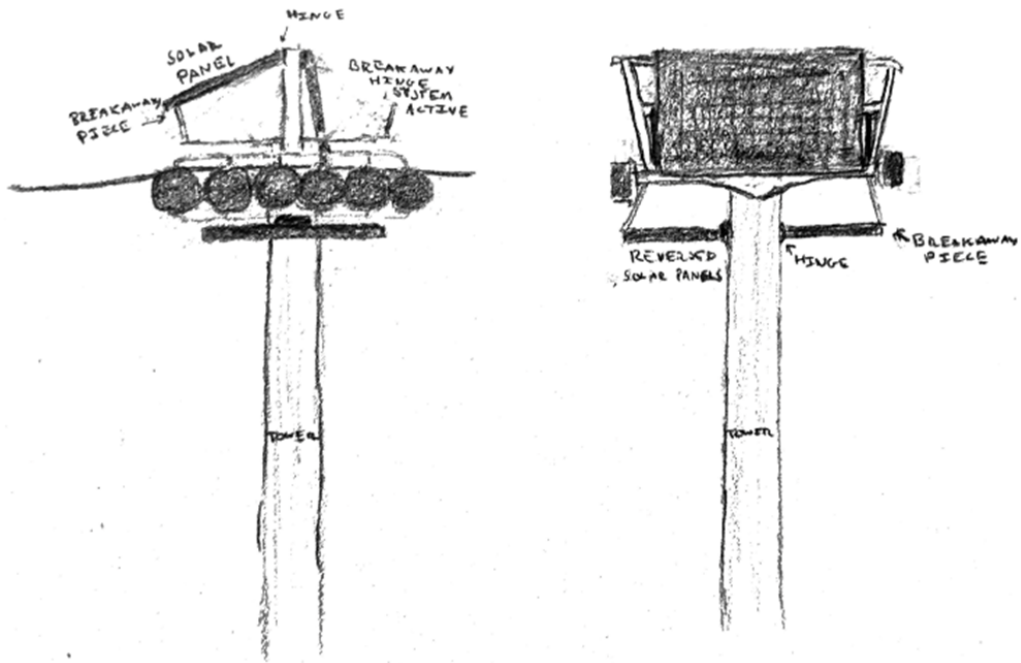


Figure 1: Original sketch of the side and front profiles of the design, with one of the top solar panels having triggered the breakaway mechanism.

Although it would usually be more efficient to put all panels in an upright position, the location of a ski slope does not lend sufficient space for this many panels. This configuration allows the panels to have a surface area that is 175% the size of the footprint, which is no larger than that of a typical lift tower. Having the solar panels extend farther from the central support tower would drastically increase the bending moments created on the lift tower as a whole, making the more compact arrangement preferable.

In order to support the extra weight, moments, and torsional forces that the panels will introduce, the central tower support has been analyzed under the new conditions and engineered accordingly. The horizontal structure atop the central tower that holds the solar panels and supports the lift cables is also redesigned in order to meet these new demands.

As is the case with any ski lift, moving people safely is the main priority of this design. In order to maintain such safety, all critical parts are designed with a factor of safety of five. Additionally, two sacrificial breakaway bolts are used in conjunction with two hinges to attach each panel to the top of the lift tower. Under excessive snow loads on a panel, the breakaway bolt is designed to fail in shear and the hinges will allow the solar panel to swing down to clear the snow. This fail-safe is only intended as an emergency measure under in the heaviest storms, where the weight from accumulating snow may compromise the integrity of the entire ski lift. Thus, the system would need to be reset and the breakaway bolt replaced by hand, but this should never occur under typical operating conditions.

Given these design considerations, this report focuses on the design of the central lift tower, the horizontal structure that holds the solar panels, the sacrificial breakaway bolt, and the hinge that allows the panels to swing if the bolt fails. All loads that each component is expected to experience are considered in the design, including static weight, dynamic forces, fatigue, torsion, and bending moments. Material selection is also considered given these loads and knowing this system is to be used outdoors and subjected to harsh weather

conditions year round.

Because the nature of this project is to generate power, and no external power will be needed for the sake of the solar array, power flow will be neglected. The power produced by the power is intended to be used throughout the rest of the ski resort to power lights, snow production, etc., in order to cut down on electricity costs and promote the use of renewable energy source. In the summer when there might not be any operations going on at a ski area, any unneeded electricity could be sold to the grid for passive income. During such times when there is no snow on the ground, the top solar panels will still be functional. The bottom ones may be dormant at this time, but because they do not requiring any energy, they can remain on the lift until the snow falls, at no cost to the owner.

2 Safety and Ethics

Ski lifts are first and foremost a way to move people. Adding solar panels to ski lift towers as researched in this report should not interfere with the ability of the lift to function as intended. Therefore, safety of those riding the lift is the main priority of the design, followed by the ability to effectively produce renewable energy for the ski area.

2.1 Structural Safety

Structural elements that people's lives depend on, such as wire in bridges and steel building structures, are commonly designed with a factor of safety value of five.² All components of this system that impact user safety will also be designed with a factor of safety of five. These critical components will include the central lift tower and the horizontal structure at its top, as these are the parts that will support the cable to hold up lift riders.

2.2 Breakaway System Safety

The sacrificial breakaway bolts attached to the solar panels are also engineered with safety in mind. A depth of half a meter of wet snow on the panels was used for the calculation of the maximum weight expected on the top of the tower. This amount of wet, high density snow covering all off the solar panels amounts to approximately $30,100\text{ N}^3$.

Failure of the bolt will allow the solar panel to swing down to shed the snow. Without this feature, it would be possible for enough snow to accumulate on the surface of the solar panels that it could impact the lift's function and potential endanger people on the lift. Once the bolt breaks and the panel swings down, it will hang in a vertical position, away from the moving parts of the lift, to prevent snow from accumulating again. All four solar panels are equipped with these bolts to fasten them on the edge opposite of the hinge.

The hinge has a factor of safety of two with regard to the breaking strength of the breakaway bolt. Because the bolt should prevent the load from exceeding this amount, the hinge only needs to be able to support slightly more force than the breakaway bolt.

2.3 Ethics

This design has the potential for positive ethical implications. The ski industry relies heavily on the power grid, which is powered almost entirely by fossil fuels. Burning fossil fuels is known to produce fossil fuels that are one of the largest contributors to global climate change. If ski areas can use designs, such as this one, to move towards using renewable energy sources, it would be a step in the right direction towards minimizing global greenhouse gas emissions, and, consequently, climate change.

3 Component Designs

In this report, there were four components that were designed. The tower and the horizontal structure were both designed in SolidWorks using FEA analysis, while the hinge and sacrificial breakaway piece were designed using hand calculations. However, the variables controlled by solar panels and snow needed to be determined first, so before the four components are explained, the solar panel and snow information are discussed.

In Figure 2, renderings of the tower, horizontal, and top solar panels are displayed. This assembly of parts is what was used for the wind simulation that will be discussed later on in section 4.



Figure 2: Tower, horizontal structure, and top solar panels modeled for the wind simulation.

3.1 Solar Panel Specifications

There are 4 solar panels used in this design, two sky-facing panels at the top and two snow-facing panels at the bottom, which are 72 cell and 60 cell PV solar panels, respectively.

The 72 cell panels are 2.1 by 1.1 m , resulting in a surface area of $2.3\ m^2$.¹ However, these top panels are tilted at an angle of 30 degrees respective to the earth, resulting in an effective surface area of $2\ m^2$. The 60 cell panels are 1.0 by 1.7 m , resulting in a surface area of $1.7\ m^2$. In total, the effective surface area of the solar panels is $7.4\ m^2$.

In terms of mass, the 72 cell panels are $23.5\ kg$ each, and the 60 cell panels are each $18\ kg$, resulting in a total solar panel mass of $83\ kg$.¹

For the power output, the 72 cell panels can produce up to $400\ W$ and the 60 cell panels can produce up to $300\ W$.⁴ However, the 60 cell panels are reversed, collecting energy from the light reflected off of the snow. Snow reflects up to 90% of sunlight, so the power output of the 60 cell panels will be $270\ W$.⁵ So under ideal conditions, which is a clear day with snow on the ground, this design will have a total power of $1,340\ W$.

Examples of 72 cell and 60 cell panels are shown in Figures 3 and 4.



Figure 3: Image of a typical 72 cell PV solar panel.¹

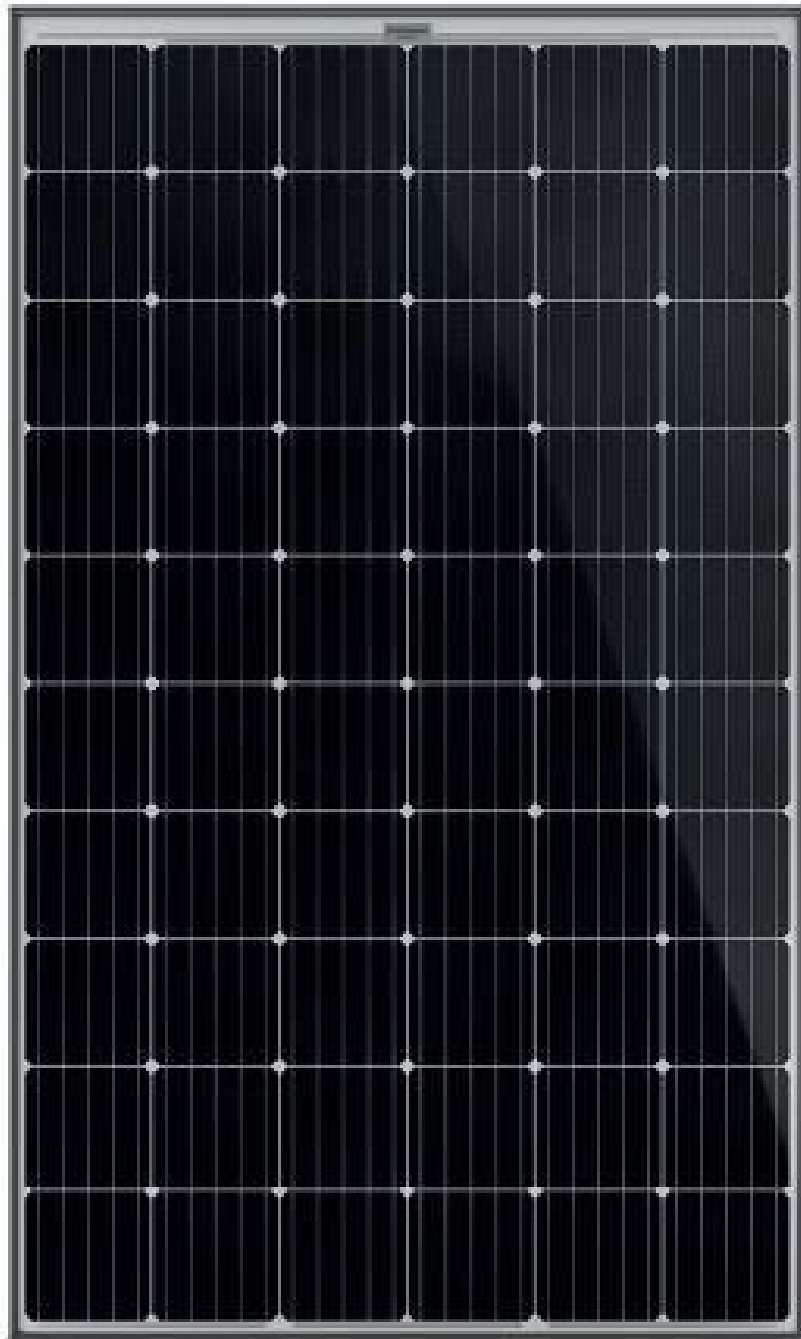


Figure 4: Image of a typical 60 cell PV solar panel.¹

3.2 Snow Load

Using a wet snow density of 830 kg/m^3 and the surface areas detailed in section 3.1, the maximum snow load could be found given the design constraint of a maximum snow of 0.5 m .³ This load was calculated to be $8,134 \text{ N}$ and $6,909 \text{ N}$ for the 72 cell panels and 60 cell panels respectively, which makes the total load of the snow and the solar panels about $8,400 \text{ N}$ and $7,100 \text{ N}$.

3.3 Tower

At the center of the lift tower design is the vertical tower, which holds the rest of the components. Normalized 4140 alloy steel is used for this part because it has high torsional fatigue strength, as well as toughness, and being subjected to the harsh climate of a ski area also makes the corrosion-resistance very beneficial.⁶

It is a hollow cylinder in shape with a diameter of 2.35 meters at the base and tapers at one degree to 1.48 m at the top. The interior diameter at the base of the tower is 1.5 m, tapering at two degrees to .49 m. Based on the $35,600 \text{ N}$ maximum overall load on the top and a factor of safety of five, the tower walls will have a thickness that increases from .425 m at the base to .5 m at the top. This calculation used the tabulated yield strength of 415 MPa for normalized 4140 and was done as part of the simulation run in SolidWorks.⁶ The thickness increasing as the diameter decrease allows for a more consistent cross-sectional area of material in the tower, which prevents the upper portion from having drastically greater values of stress because of the smaller area of material holding the same load. At the base, the tower is bolted to a concrete foundation that is considered static for the sake of this design. The design of the tower is detailed in Figure 5.

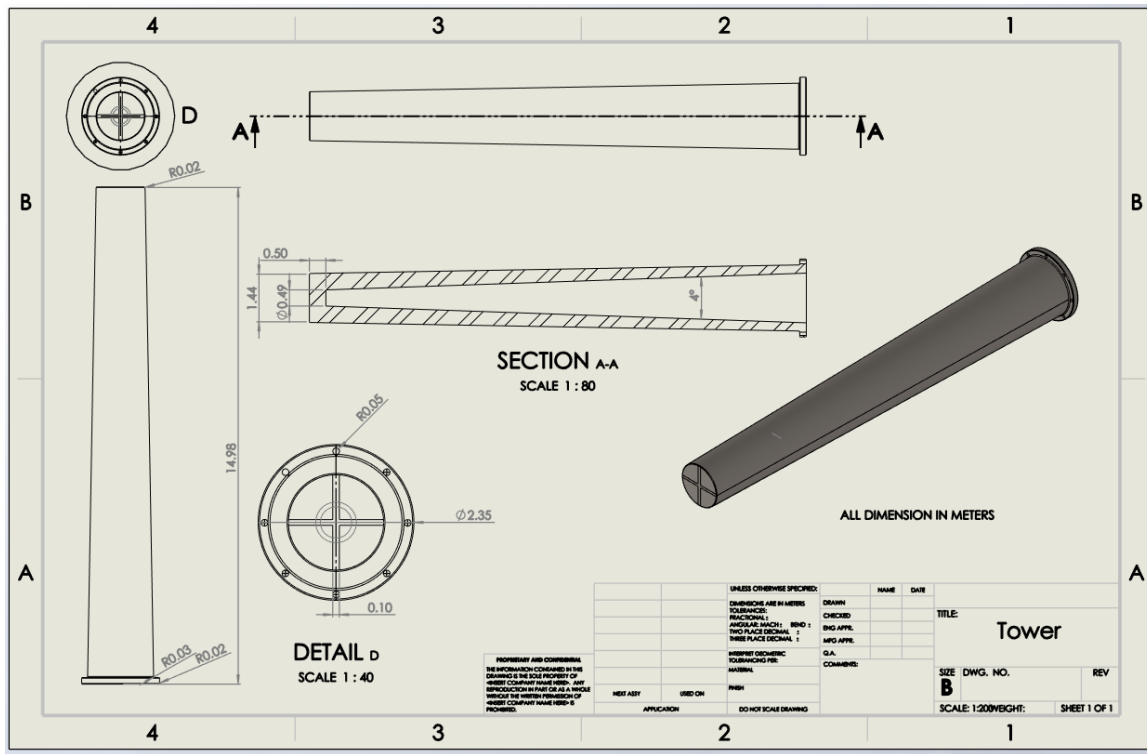


Figure 5: Drawing of tower. Units are in meters.

3.4 Horizontal Structure

On top of the central lift tower, a horizontal structure holds all of the other lift components in place. The dimensions of this structure are detailed in Figure 6.

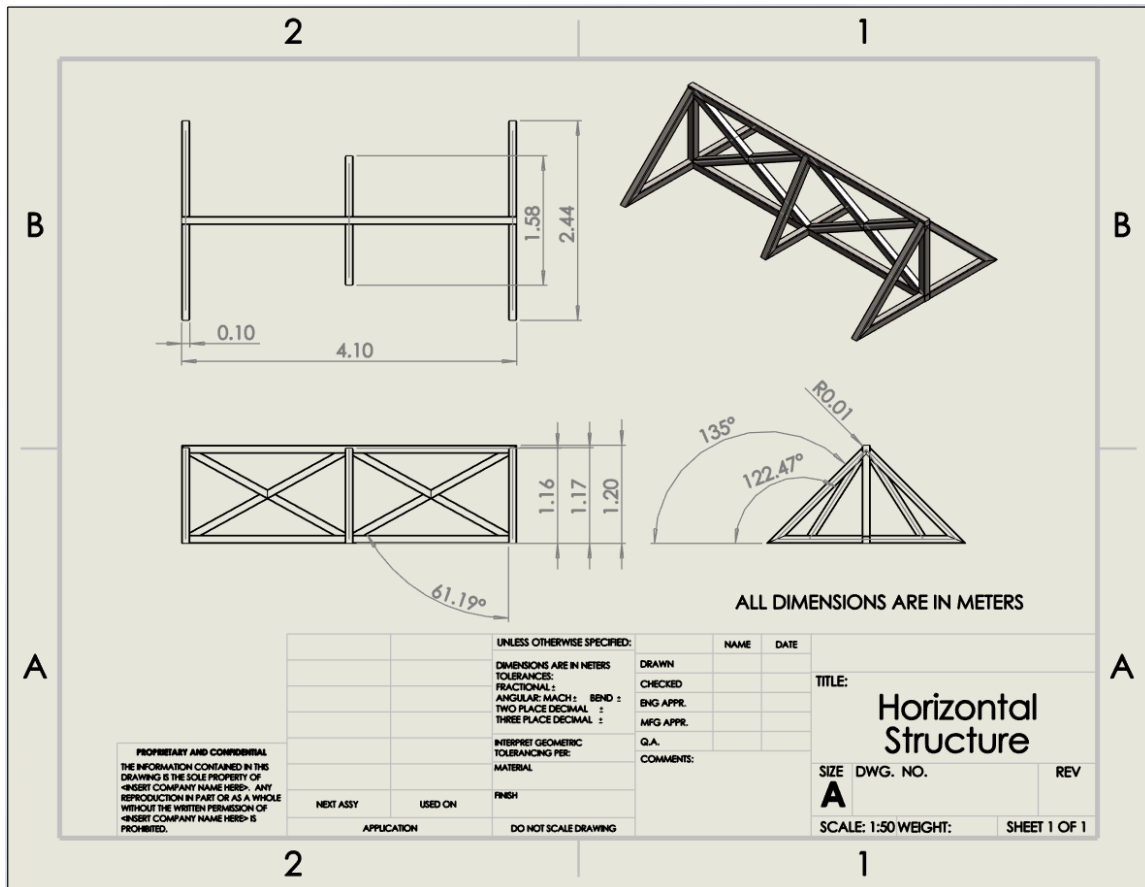


Figure 6: Drawing of horizontal structure. Units are in meters.

Seen in Figure 1, the top two solar panels attach to it at an angle and the bottom two are held horizontally below it, all via hinges and breakaway bolts. It is also made from normalized 4140 steel in order to be tough, corrosion-resistant, and have a high fatigue strength. Unlike the tower, which is a hollow cylinder, this is a framework made from welded beams. The welded beams allow for strength and rigidity, while being significantly lighter than a solid piece of steel for the entire structure. Additionally, repairs and installation are made easier since this portion is welded together. A cross section of the beam used in the horizontal structure is displayed in Figure 7.

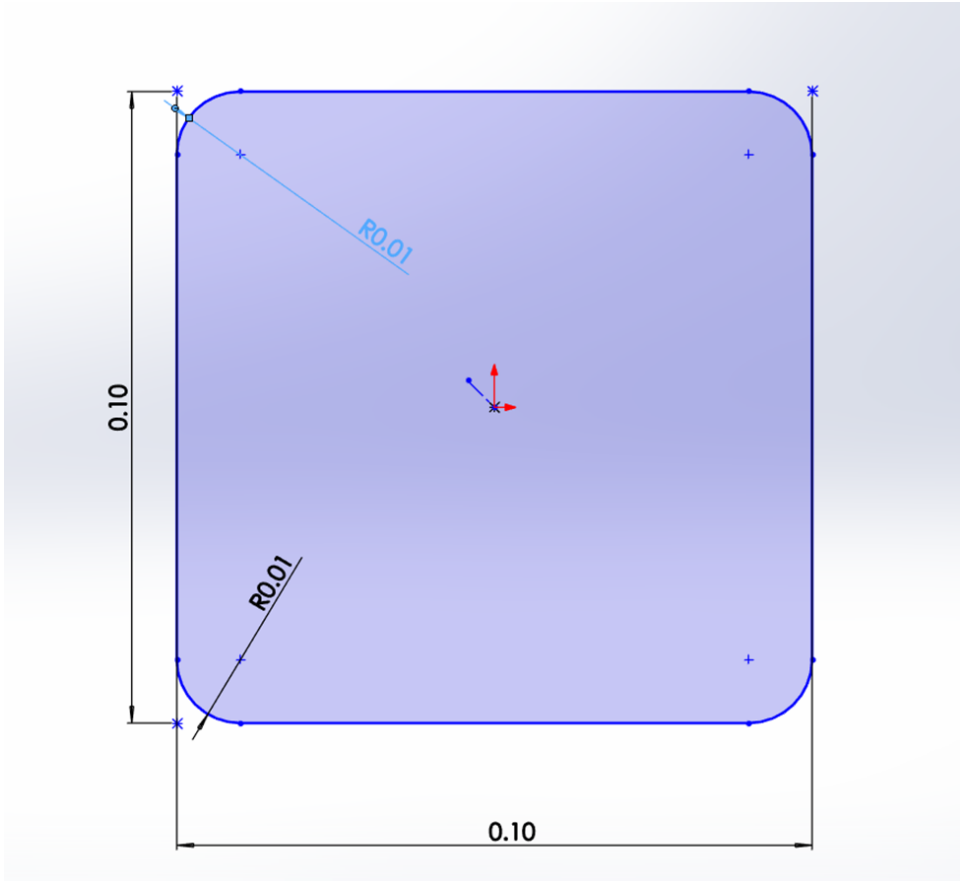


Figure 7: Cross section of the beam for the horizontal structure. Units are in meters.

The horizontal must be able to hold the static load from the panels in addition to the load from the lift chairs and people suspended by the cable it is supporting. This total weight is estimated at 35,600 N , but the factor of safety of five means the structure is designed to hold 142,200 N .

3.5 Hinge and Breakaway System

A sketch of the principles behind this breakaway system are detailed in Figure 8.

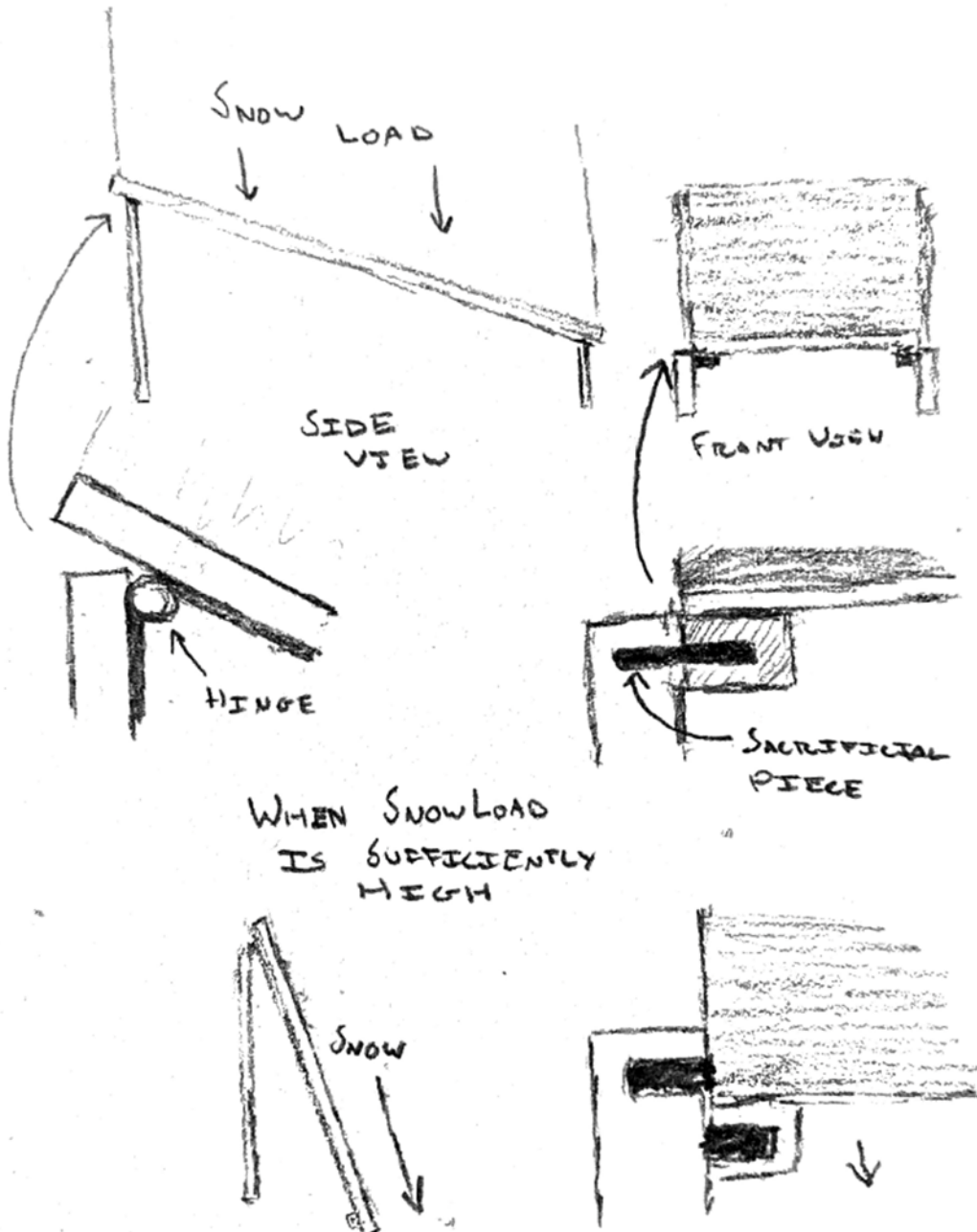


Figure 8: Sketch of breakaway system.

The sacrificial pieces used in the breakaway system were designed to be made out of ABS plastic as it is cheap and simple pieces are easy to produce. This material has a shear strength of 3.6 MPa .⁷ Using the snow loads calculated in section 3.2 and the weights of the solar panels, Equation 1 was used to calculate the required radii of the sacrificial breakaway piece. The load for the pieces are divided by 4 because there are 2 sacrificial pieces holding up half of the load.

$$r_{breakaway} = \sqrt{\frac{W_{snow} + W_{panel}}{4 \cdot 3.6 \text{ MPa} \cdot \pi}} \quad (1)$$

Completing those calculations results in the sacrificial pieces for the 60 cell panels having a radius of 1.25 cm and the sacrificial pieces for the 72 cell panels having a radius of 1.36 cm .

However, as the temperature drops, so does the shear strength of ABS, reaching 3.4 MPa at a temperature of -40 degrees Fahrenheit (which is also -40 degrees Celsius).⁷ This change greatly reduces the depth of snow at which the sacrificial pieces fail, with them failing at a depth of about 0.09 m and 0.11 m for the 72 cell panels and the 60 cell panels respectively.

While this seems like a massive difference, all of the calculations involving snow have been using the maximum density of wet snow. Dry and powdery snow is much lighter, with a density as low as 50 kg/m^3 , which is over 16 times less dense as the value of wet snow being used in these calculations, and is the type of snow that usually falls at colder temperatures. The type of snow that falls at temperatures of -40 degrees Celsius is certainly dry and powdery.



Figure 9: Production hinge from Gatemaster Locks used as a reference.⁸

The hinge component was designed out of cold rolled 1018 steel with an inorganic zinc coating to prevent corrosion. 1018 steel was chosen because of its strength and use in bolts and fasteners. A major downside of cold rolled 1018 steel is the fact that it has very low resistance to corrosion.⁹ The inorganic zinc coating that will be applied to the hinge is the coating that is used in many industrial steel applications that require low corrosion, such as the production of ships.¹⁰ There are two hinges attached to each panel, located on the side nearest the ski tower main pole.

The diameter of the pin in double shear, perpendicular to the bolt section, was calculated to be 3 *mm*. Equations 2 and 3 were used in order to determine this value. The shear strength used was that of cold rolled 1018 steel, being 296.5 *MPa*.⁹ The load used was double the load causing the sacrificial pins to break on the large solar panel. This provides the hinge with a factor of safety of two for the large panels, and slightly over two for the small panels. The decision was made to use the same hinge for both solar panels in order to increase the ease of production by requiring less unique components.

$$\tau_{bolt} = \frac{2P}{\pi d^2} \quad (2)$$

$$d = \sqrt{\frac{2 * P}{\pi \tau}} \quad (3)$$

The next part of the hinge that was designed was the bolt section. This is the part that will screw into the solar panel itself, holding it up when in use and holding the weight of the panel when dangling if the sacrificial pins snap. The bolt was also chosen to be made out of cold rolled 1018 steel with organic zinc coating. The same reasoning applies to this piece that was used on the pin in double shear. The strength of the 1018 steel and corrosion resistance from the coating provide both the safety and longevity needed for the component.

The diameter of the bolt section of the hinge was calculated using equations 4 and 5. Once again, the force required to break the sacrificial pins on the large solar panel was used, since it should be the largest force the hinges are exposed to. The shear strength was also previously mentioned as 296.5 *MPa*. Using these values it was determined that the appropriate diameter of the bolt section is three millimeters. This is with a factor of safety of slightly over two.

$$\tau = \frac{F}{A} = \frac{4F}{\pi d^2} \quad (4)$$

$$d = \sqrt{\frac{4F}{\tau\pi}} \quad (5)$$

Finally, the tensile stress of the bolt section of the hinge was calculated with the previously determined diameter of three millimeters. This was done in order to prove that the hinge will not fail if the sacrificial pins snap and the panels swing down. The yield tensile strength was determined with equation 6 below, and found to be 5075.18 N. Dividing this by the force of the solar panel that will be hanging if the sacrificial pins snap, and multiplying by two because there will be two hinges holding up each panel, provides a factor of safety of 44. This proves the diameter needed to maintain the proper factor of safety for the shear forces, while limiting material used, is well within the safety specifications for tensile strength. The calculations were again done only on the larger solar panel, meaning the factor of safety on the smaller panels will be even greater.

$$F_{yield} = \sigma * A \quad (6)$$

4 Finite Element Analysis

SolidWorks finite element analysis software (FEA) was used to design and analyze the loads on the tower and horizontal structure. Von Mises calculations were used, given that they yield more accurate maximum stress values than other stress theories and formulas. All of the FEA results figures can be found in the appendix, section 5.2.

4.1 Tower FEA

The tower design started with a defined height, outer diameter, and taper, and the wall thickness was adjusted accordingly based on how the normalized 4140 steel was effected by the 35,600 N (8,000 lbs) load seen in figure 17. This leads to a maximum compressive stress of about 477 kPa at the top of the tower where the horizontal structure is attached. Given that 415 MPa is the yield strength of the steel used, there should be no worries about the tower failing, save for any unexpected circumstances such as earthquakes. A factor of safety of five was also simulated on the main shaft of the tower, seen in figures 18, 20, and 22. Displacement is shown to be insignificantly small, at around 0.009 mm. The Von Mises stresses are around 3 orders of magnitude below the yield stress, meaning there is now risk of the tower yielding under the given loads.

The mesh information of the tower is displayed in Figure 10.

Mesh Details	
Study name	Static 1* (-Default-)
Details	Mesh type
	Solid Mesh
Mesher Used	Blended curvature-based mesh
Jacobian points for High quality mesh	16 points
Max Element Size	0.523605 m
Min Element Size	0.0261803 m
Mesh quality	High
Total nodes	76963
Total elements	47288
Maximum Aspect Ratio	25.018
Percentage of elements with Aspect Ratio < 3	98.4
Percentage of elements with Aspect Ratio > 10	0.0233
Percentage of distorted elements	0
Number of distorted elements	0
Time to complete mesh(hh:mm:ss)	00:00:06
Computer name	XPS15-LECHAILL

Figure 10: Mesh information of the tower.

4.2 Horizontal Structure FEA

A 4 *m* length, 1.1 *m* height, and 4140 steel material were initially defined to design the horizontal structure. The shape is a product of reinforcing the weak areas from early loading simulations. All welded corners are filleted to minimize stress concentrations and to simplify the calculations done by the software.

The mesh information of the tower is displayed in Figure 11.

Mesh Details	
Study name	Static 1 (-Default<As Machined>-)
DetailsMesh type	Beam Mesh
Total nodes	318
Total elements	306
Time to complete mesh(hh:mm:ss)	00:00:02
Computer name	XPS15-LECHAILL

Figure 11: Mesh information of the structure.

Figure 12 shows the displacement under 35,600 N (8,000 lbs), which is the maximum expected load on the structure. Figure 13 displays the stress under the same load. To demonstrate the factor of safety, Figure 12 shows the displacement under five times the maximum load, and Figure 13 depicts the corresponding stresses. As can be seen in these last two images, the structure will not fail under five times the maximum load (178,000 N or 40,000 lbs), proving that the factor of safety holds.

4.3 Wind Simulation

For the wind simulation, the top solar panels were added to the structure. The bottom ones were not as they are parallel to the flow so any forces caused by the fluid on the design can be assumed to be negligible. The working fluid was air, with an inlet velocity of 45

m/s , which is about 100 mph. This value was given by the Director of Technical Services (Ropeway Engineering) from the National Ski Areas Association, Michael Lane. Figure 24 displays the forces on the tower caused by the flow and Figure 25 displays the shear stress on the tower caused by the flow.

5 Appendix

5.1 Sample Calculations

Radius of sacrificial piece for the 72 cell solar panel:

$$r_{breakaway} = \sqrt{\frac{W_{snow} + W_{panel}}{4 \cdot 3.6 \text{ MPa} \cdot \pi}}$$
$$r_{breakaway} = \sqrt{\frac{8400}{4 \cdot 3.6 \text{ MPa} \cdot \pi}} = 0.0136 \text{ m} = 1.36 \text{ cm}$$

Radius of sacrificial piece for the 60 cell solar panel:

$$r_{breakaway} = \sqrt{\frac{W_{snow} + W_{panel}}{4 \cdot 3.6 \text{ MPa} \cdot \pi}}$$
$$r_{breakaway} = \sqrt{\frac{7100}{4 \cdot 3.6 \text{ MPa} \cdot \pi}} = 0.0125 \text{ m} = 1.25 \text{ cm}$$

Diameter of double shear part of the hinge:

$$d = \sqrt{\frac{2 * P * FOS}{\pi \tau}}$$
$$d = \sqrt{\frac{2 * 2033.5 * 2}{\pi (296.5 * 10^6)}} = 0.002955 \text{ m} = 2.955 \text{ mm}$$

Diameter of bolt section of the hinge:

$$d = \sqrt{\frac{4F * FOS}{\tau\pi}}$$

$$d = \sqrt{\frac{4 * 2033.5 * 2}{296.5 * 10^6 * \pi}} = 0.004179mm = 4.179m$$

Yield tensile force on the bolt section of the hinge:

$$F_{yield} = \sigma * A = 370.25 * 10^6 * \pi * 0.0020895^2 = 5075.18N$$

5.2 Finite Element Analysis Results

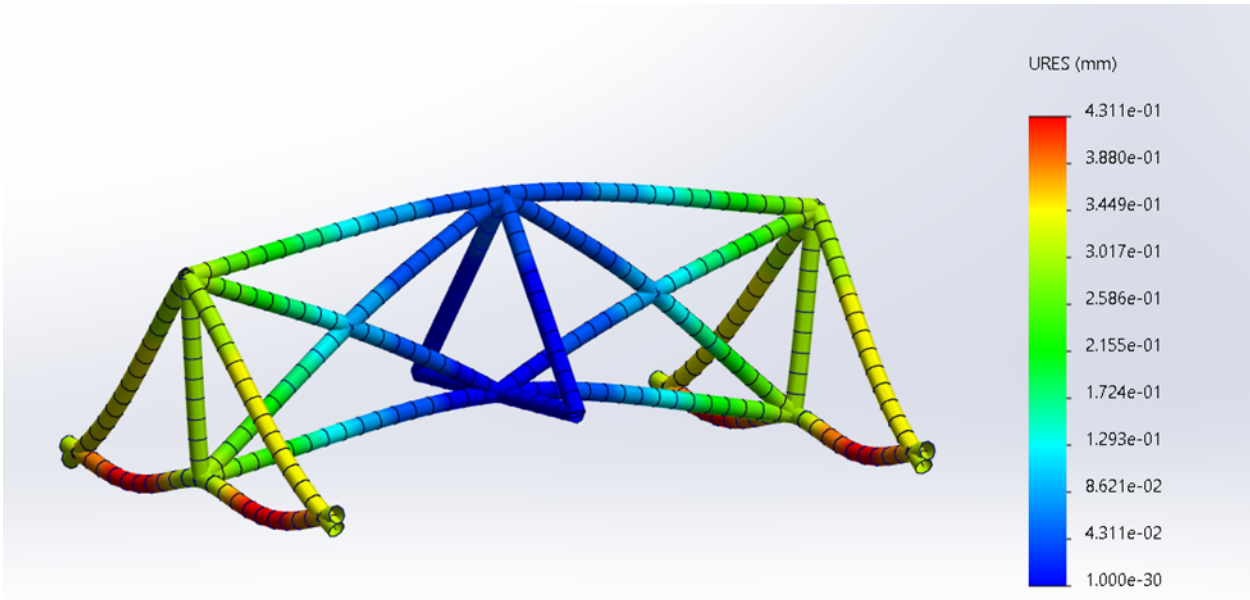


Figure 12: Displacement figure for the horizontal structure under 8000 lbs of weight. Displacement is exaggerated to be easily seen.

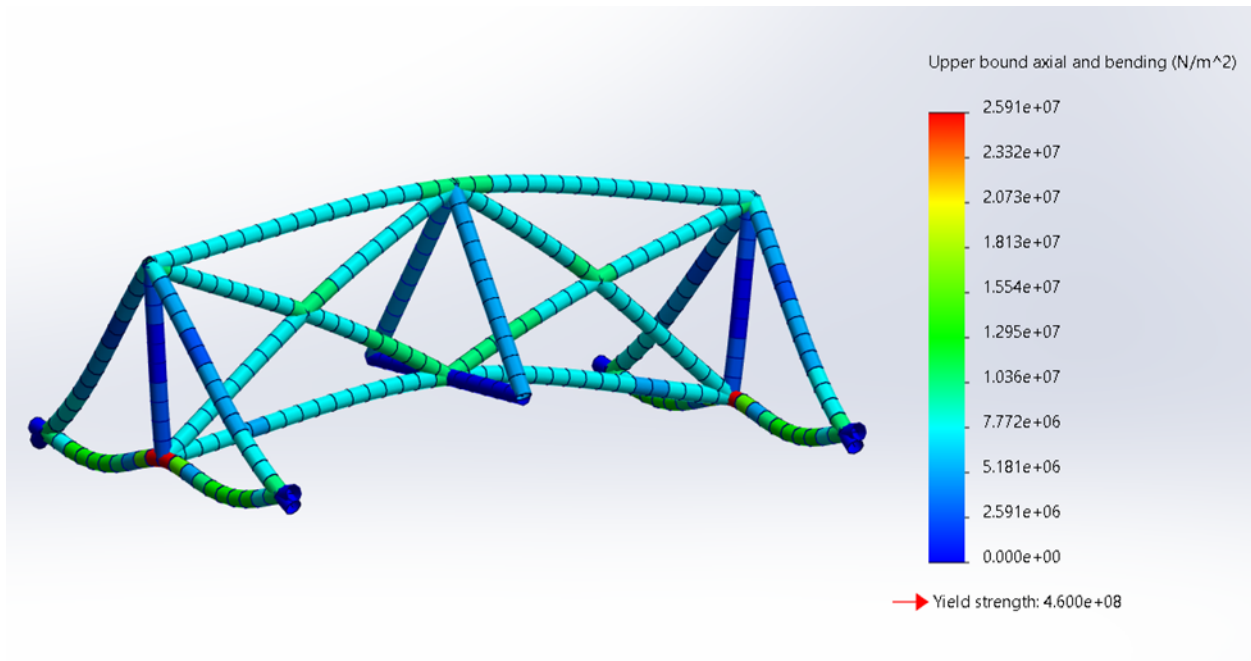


Figure 13: Stress figure for the horizontal structure under 8000 lbs of weight. Displacement is exaggerated to be easily seen.

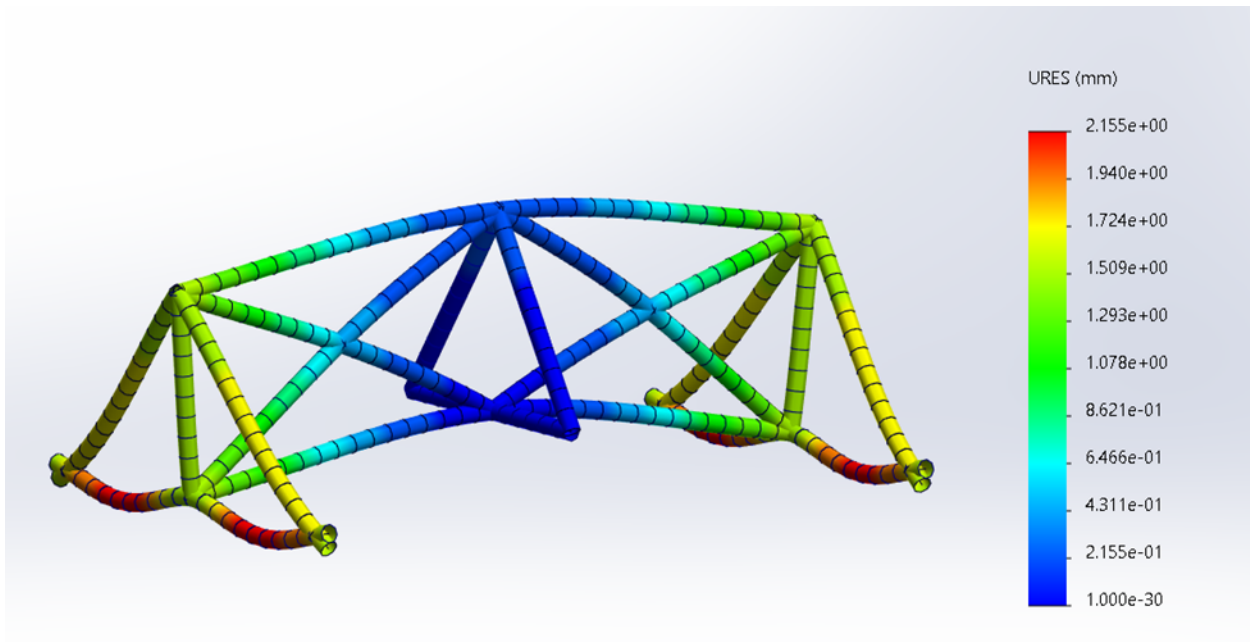


Figure 14: Displacement figure for the horizontal structure under 40000 lbs of weight. Displacement is exaggerated to be easily seen.

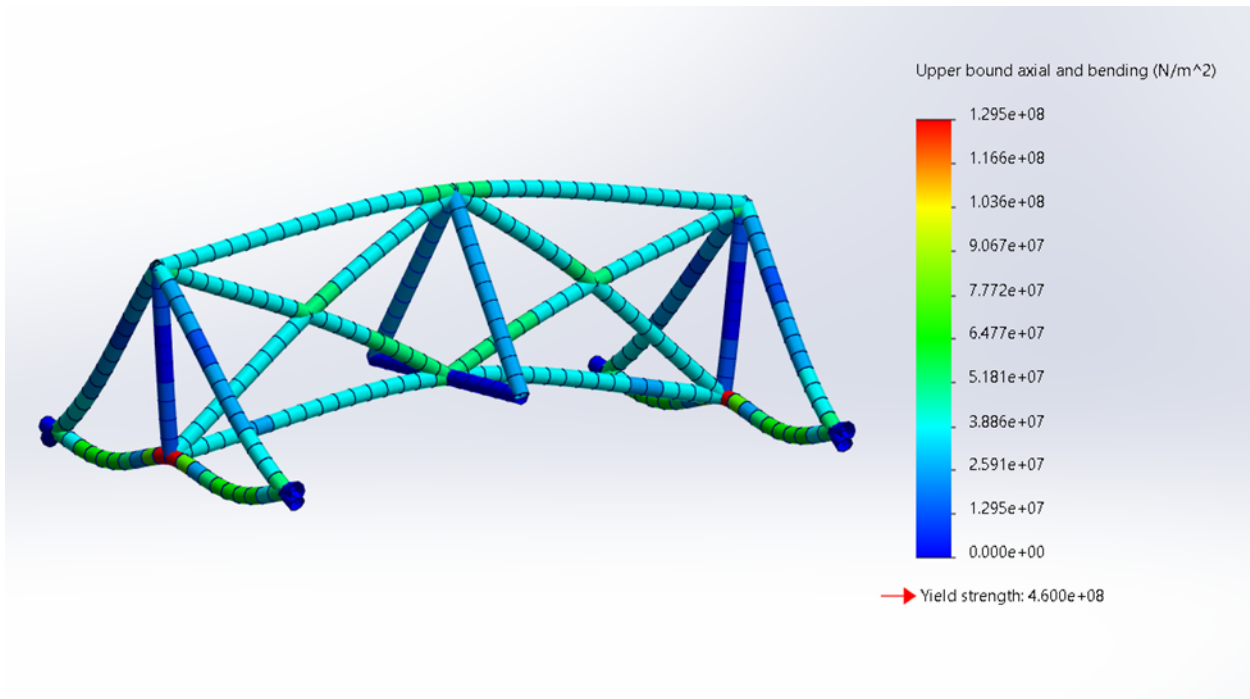


Figure 15: Stress figure for the horizontal structure under 40000 lbs of weight. Displacement is exaggerated to be easily seen.

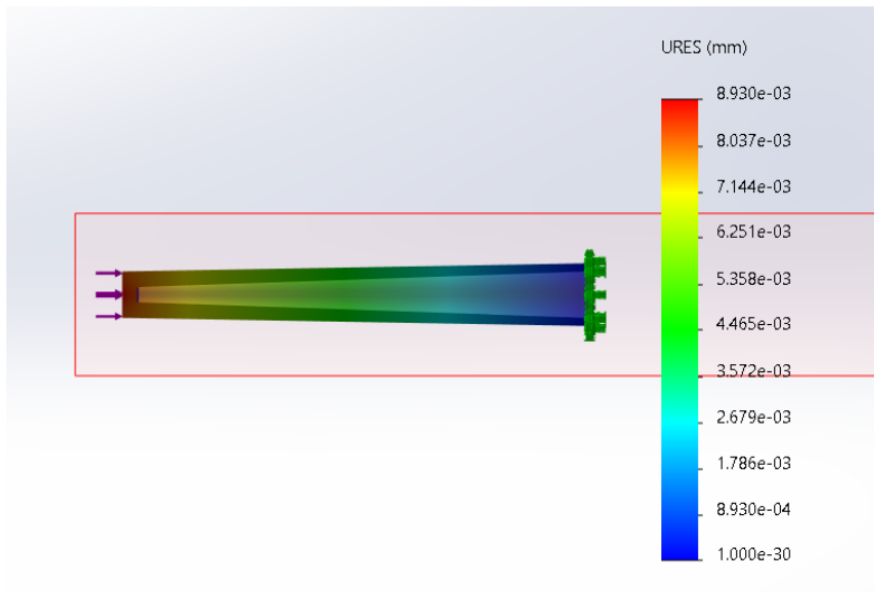
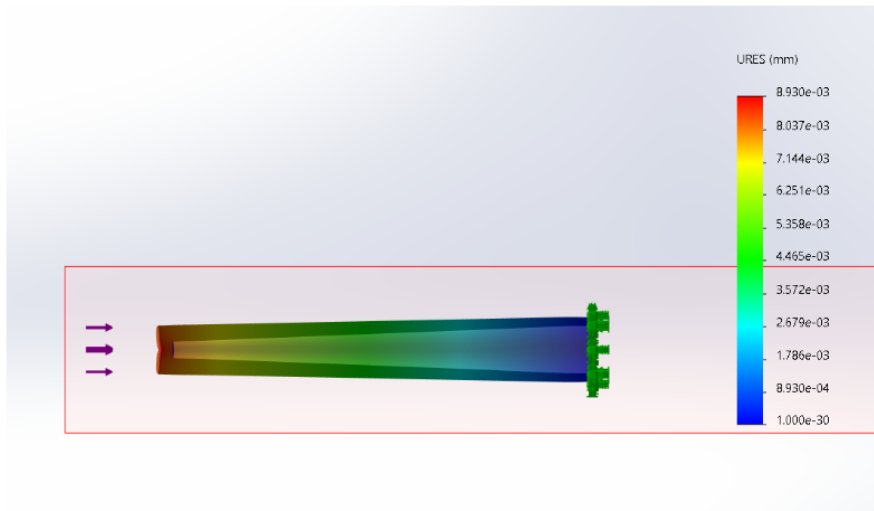


Figure 16: Displacement figure for the tower under 40000 lbs of weight. The bottom figure shows exaggerated results.

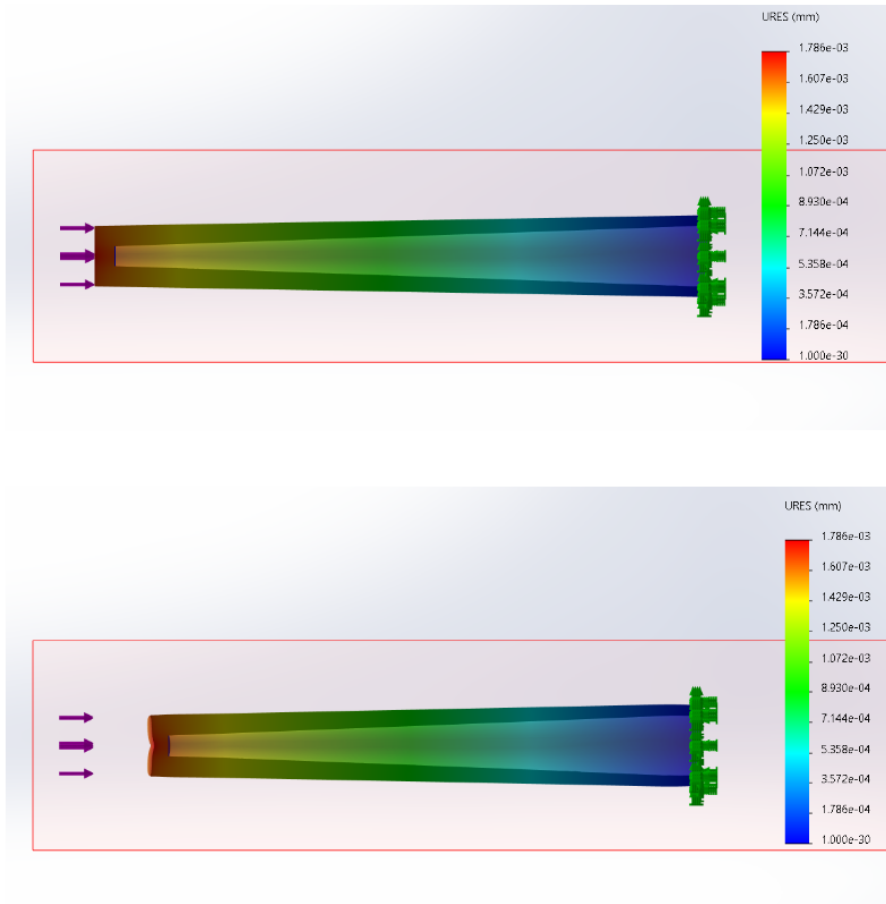


Figure 17: Displacement figure for the tower under 8000 lbs of weight. The bottom figure shows exaggerated results.

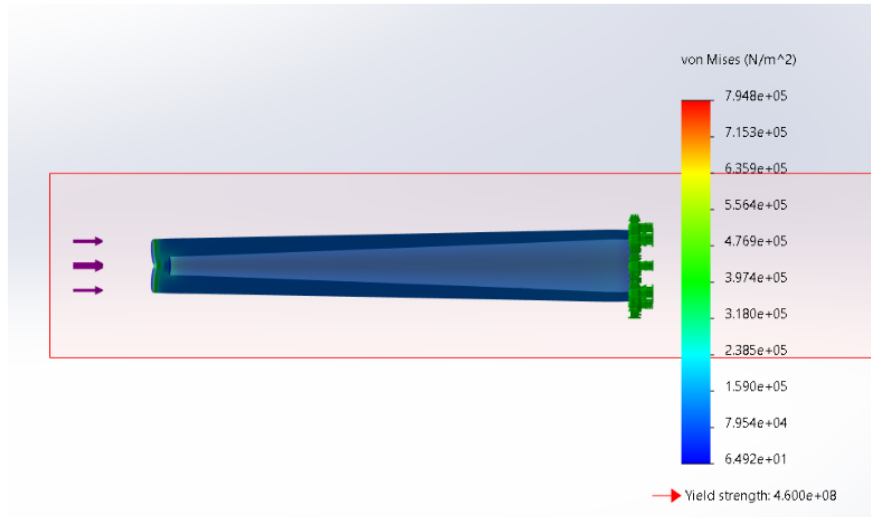
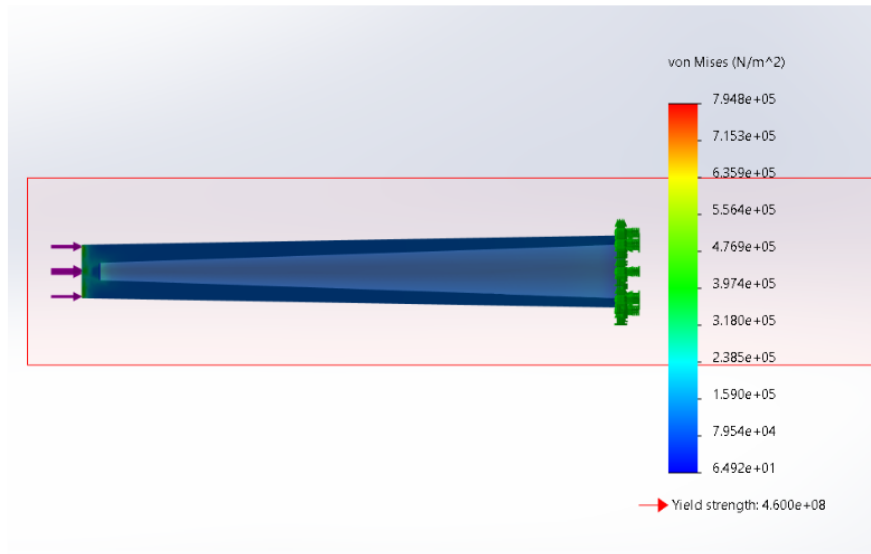


Figure 18: Von Mises figure for the tower under 40000 lbs of weight. The bottom figure shows exaggerated results.

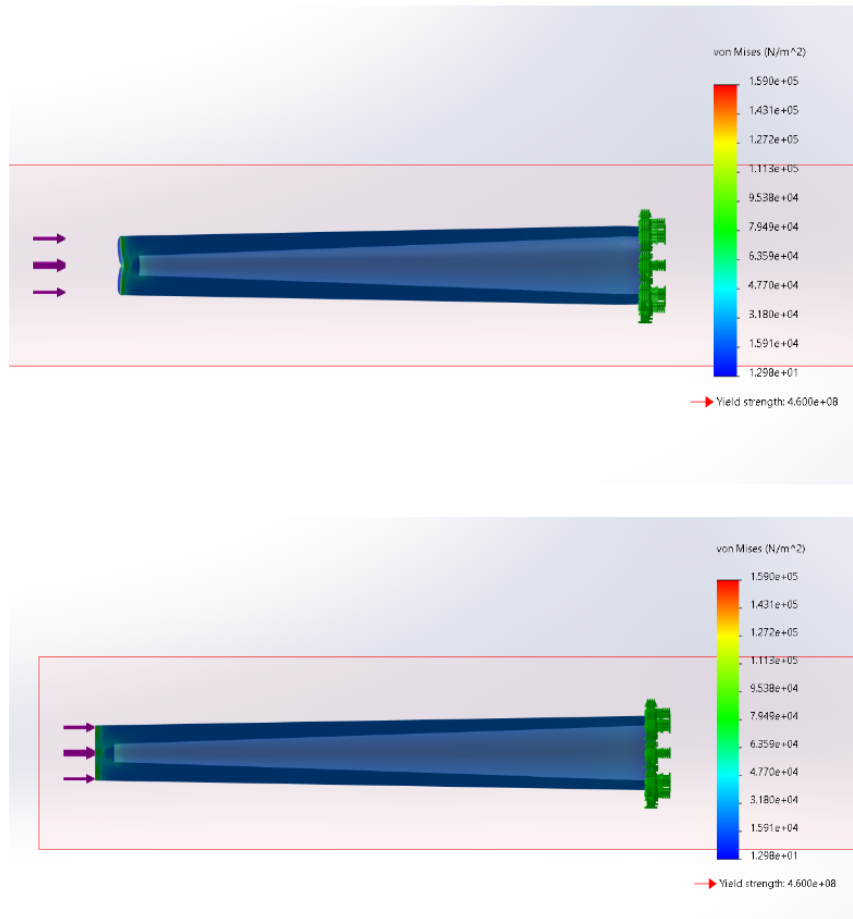


Figure 19: Von Mises figure for the tower under 8000 lbs of weight. The bottom figure shows exaggerated results.

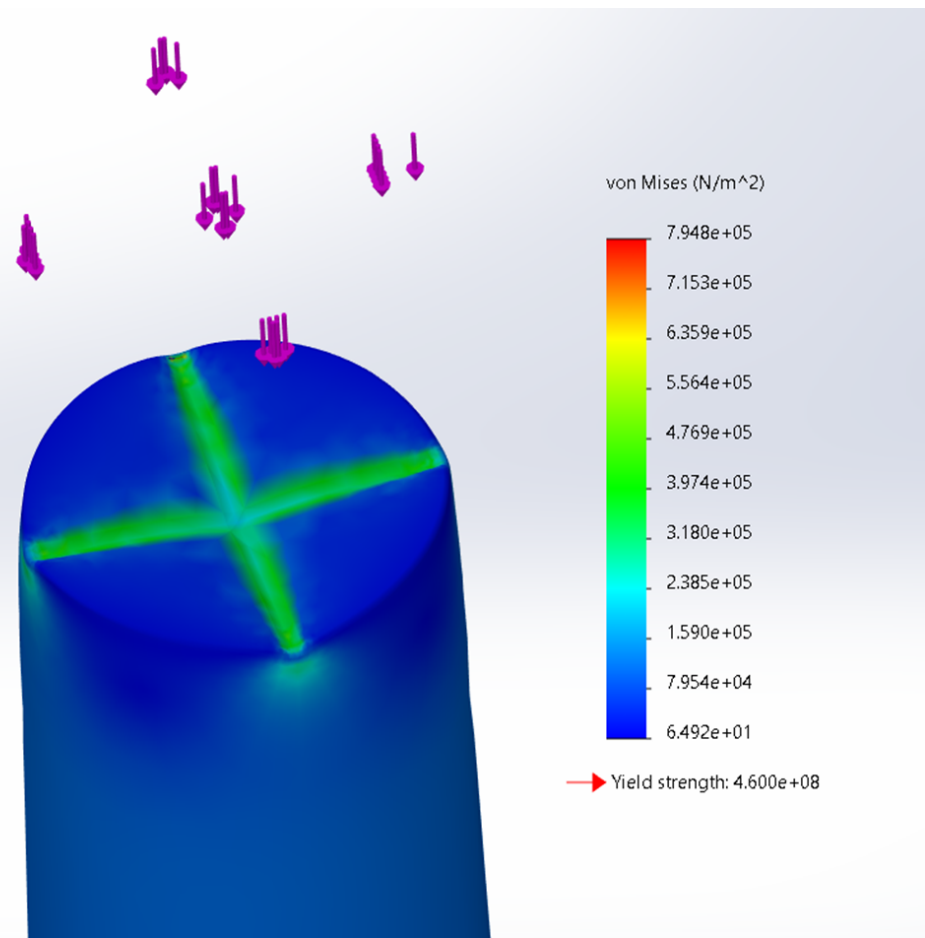


Figure 20: Von Mises figure for the top of the tower under 40000 lbs of weight. Displacement is exaggerated to be easily seen.

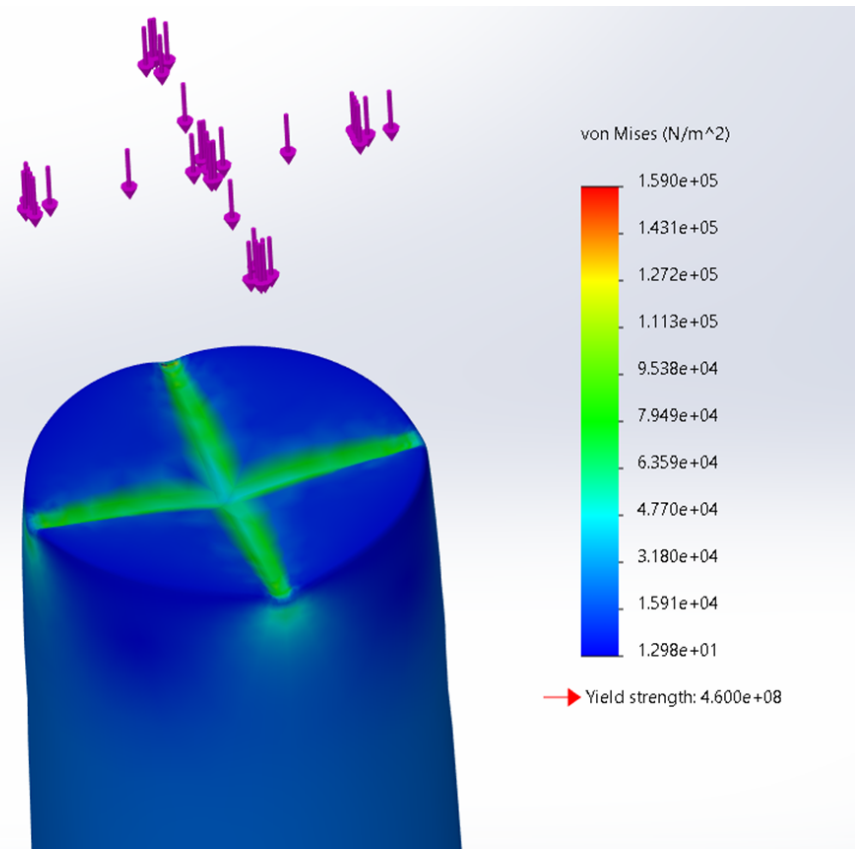


Figure 21: Von Mises figure for the top of the tower under 8000 lbs of weight. Displacement is exaggerated to be easily seen.

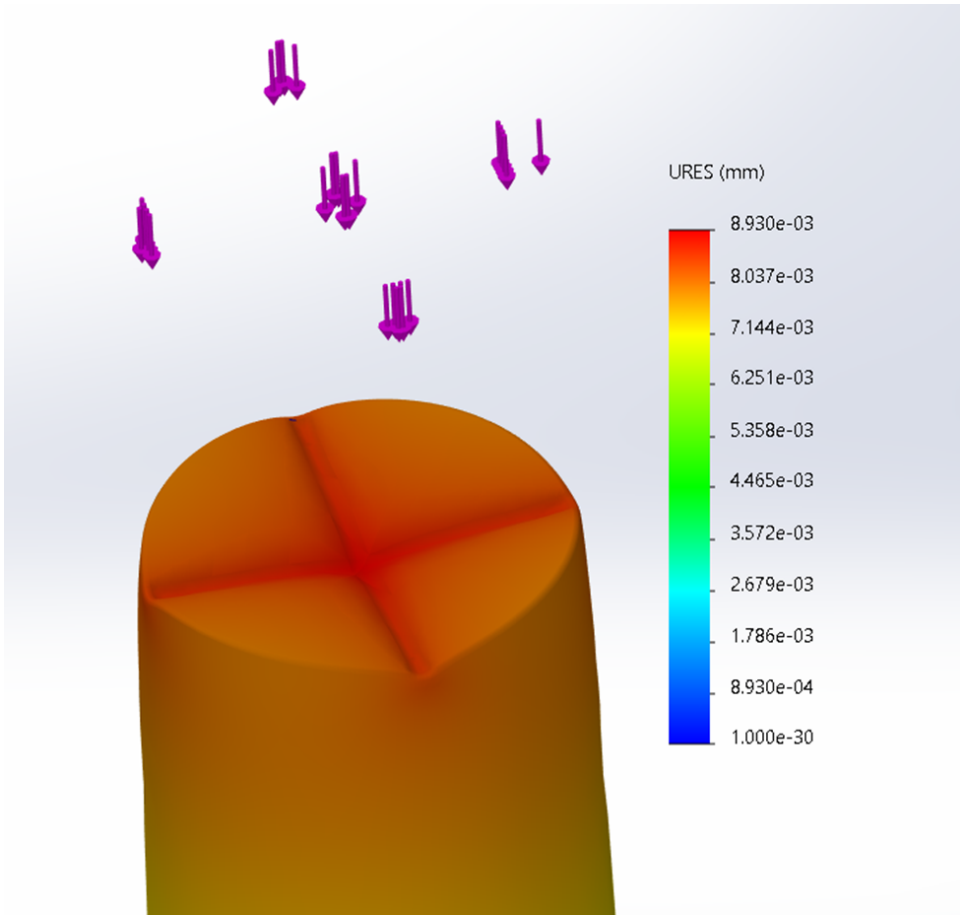


Figure 22: Displacement figure for the top of the tower under 40000 lbs of weight. Displacement is exaggerated to be easily seen.

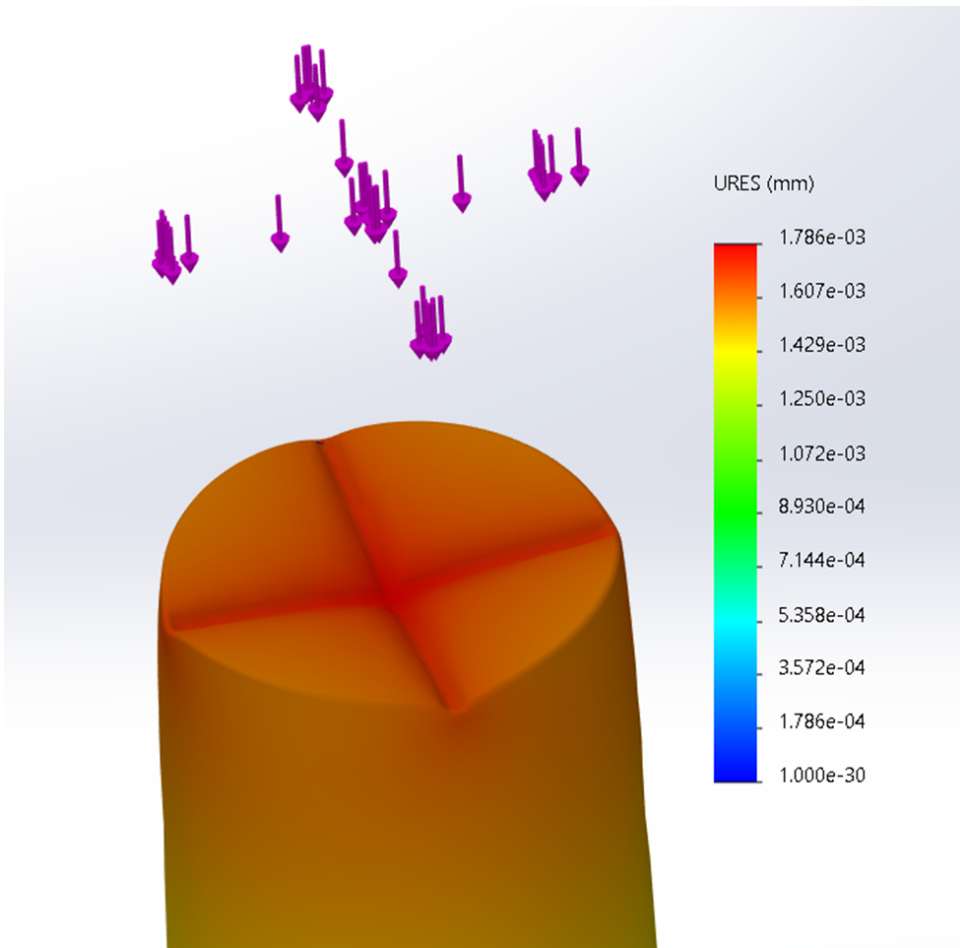


Figure 23: Displacement figure for the top of the tower under 8000 lbs of weight. Displacement is exaggerated to be easily seen.

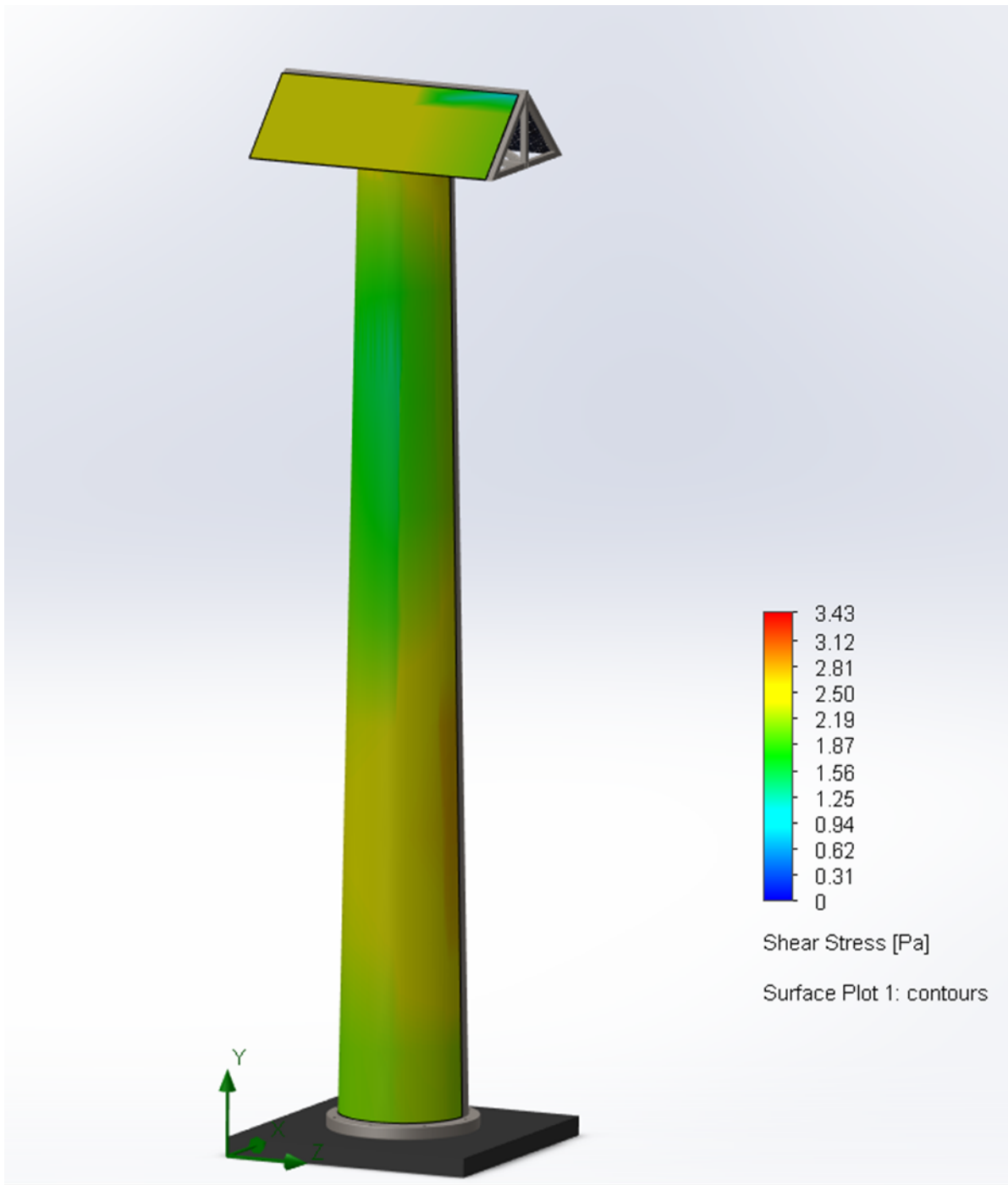


Figure 24: Distributed force from the wind on the tower.

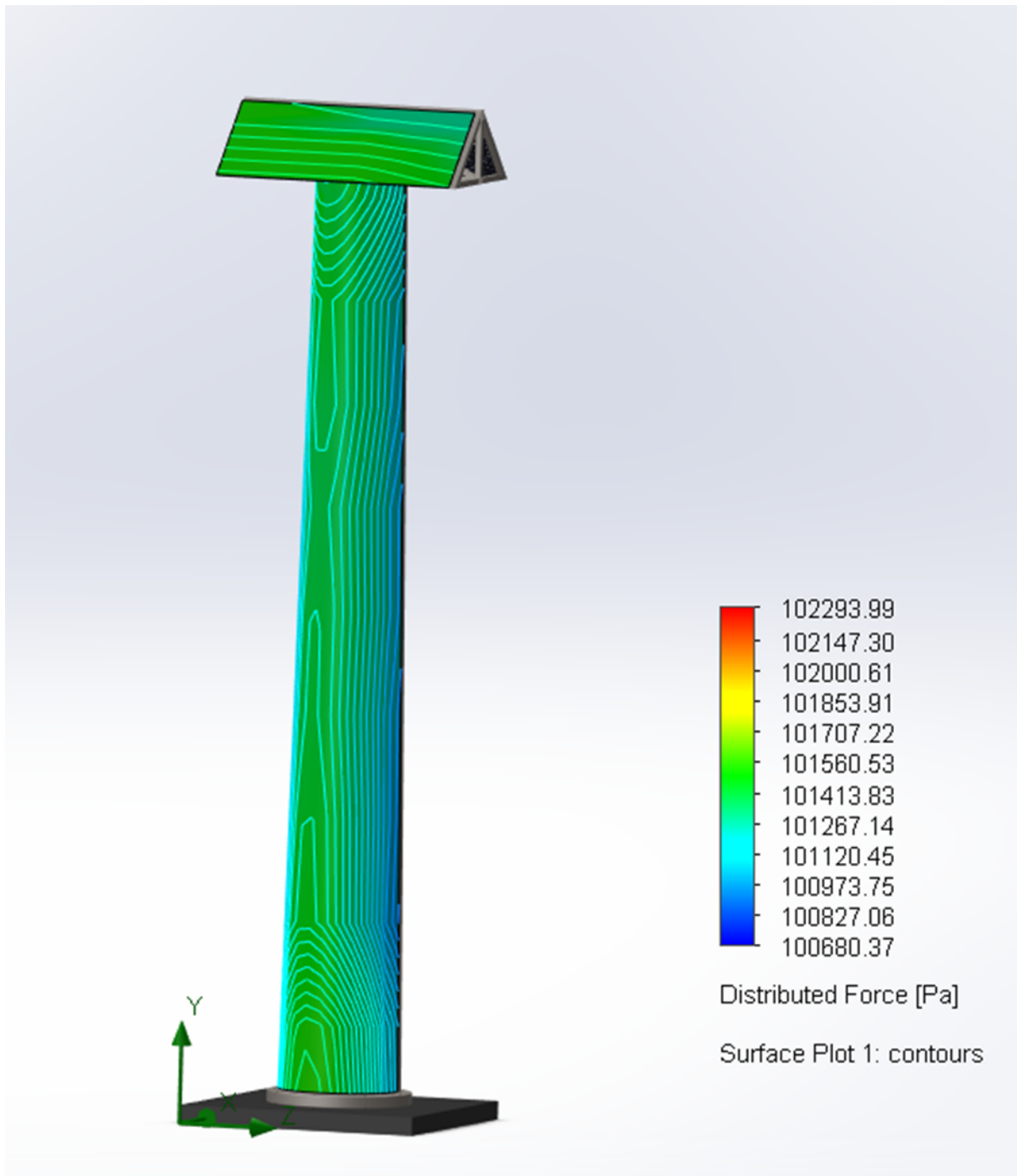


Figure 25: Shear stress from the wind on the tower.

6 Bibliography

References

- [1] J. Sykes, “Solar panel sizes and dimensions,” Solar Choice, <https://www.solarchoice.net.au/solar-panels/sizes> (accessed Apr. 19, 2024).
- [2] “Factors of safety - fos,” Engineering ToolBox, <https://www.engineeringtoolbox.com/factors-safety-fos-d-1624.html> (accessed May 2, 2024).
- [3] Joe Sexton, “Snow weight calculator,” Inch Calculator, <https://www.inchcalculator.com/snow-weight-calculator/> (accessed May 1, 2024).
- [4] “How much energy do solar panels produce?,” Solar Technologies, <https://solartechologies.com/how-much-energy-do-solar-panels-produce/> (accessed May 2, 2024).
- [5] “Dusting the virtues of snow,” Earth Observatory, <https://earthobservatory.nasa.gov/features/DirtySnow/page2.php> (accessed Apr. 19, 2024).
- [6] “4140 Alloy Steel: Uses, composition, properties,” Xometry RSS, <https://www.xometry.com/resources/materials/4140-alloy-steel/> (accessed May 2, 2024).
- [7] J. G. Quini and G. Marinucci, “Polyurethane structural adhesives applied in automotive composite joints,” Materials Research, vol. 15, no. 3, pp. 434–439, May 2012. doi:10.1590/s1516-14392012005000042

[8] “The industrial heavy-duty Hinge,” Gatemaster Locks, <https://www.gatemasterlocks.com/industrial-heavy-duty-hinge-superhinge/> (accessed May 2, 2024).

[9] “Carbon-steel 1018 product guide from online metals,” OnlineMetals, <https://www.onlinemetals.com/en/product-guide/alloy/1018> (accessed May 2, 2024).

[10] “Corrosion resistant coatings for steel – types and uses,” Secoa Metal Finishing, <https://secoatech.com/corrosion-resistant-coatings-for-steel-types-and-uses/> (accessed May 2, 2024).